DOI: 10.13009/EUCASS2023-636
Aerospace Europe Conference 2023 – 10TH EUCASS – 9TH CEAS

Effects of Flexibility on Reorientation of Multibody Spacecraft Using Internal Torques

Behrad Vatankhahghadim[⋆†] *and Marco Lovera*[⋆]
[⋆]*Politecnico di Milano*
Via Giuseppe La Masa 34, 20156, Milan, Italy
behrad.vatankhahghadim@polimi.it · marco.lovera@polimi.it
[†]Corresponding author

Abstract

The effects of flexibility on attitude control using internal torques that change the shape of multibody spacecraft is studied. Conservation of angular momentum provides a nonholonomic constraint that can be leveraged to relate attitude changes to those of joint angles, assumed to be controllable via internal torques dictating the angles' accelerations. Open-loop torques can be subsequently designed using a profile in the shape space, the attitude change from which can be numerically computed in advance. This paper shows that even small amounts of flexibility can significantly alter the attitude changes, but such influences could be minimized by conducting slower manoeuvres.

1. Introduction

The problem treated in this paper is that of reorientation via shape change in the context of multibody spacecraft, in particular in the presence of flexibility effects. Examples of earlier works on a similar problem involving rigid bodies were presented by Krishnaprasad,[4] Sreenath,[9] Walsh and Sastry,[12] Rui *et al*,[8] and Cerven and Coverstone,[1] among others. It is also interesting to note that the overall control mechanism via shape change is inspired by the so-called falling cat problem related to the reorientation manoeuvres performed by cats when released upside down, studied by Kane and Scher,[2] for example: a phenomenon that finds applications in other contexts as well, such as astronaut reorientation and springboard diving.

Whereas the research in the area of attitude control via shape change has thus far focused on rigid systems, the present document introduces flexibility and explores the effects of the appendages' deflections. The kinematics and dynamics of the flexible problem are based on the mathematical derivations presented elsewhere by this paper's authors, Vatankhahghadim and Lovera,[11] along with further references to the relevant literature and using a control mechanism similar to that by Walsh and Sastry.[12] The control approach is based on calculating the geometric phase for a given profile, that is, determining the amount of change in the configuration space (overall attitude) resulting from a given profile in the shape space (defined by the joint angles).[4] Other applications of geometric phases in the context of spacecraft attitude control can be found in the works of Krishnaprasad and Yang,[5] Sreenath,[10] Reyhanoglu and McClamroch,[7] and Narikiyo and Ohmiya,[6] among others. Also relevant is the in-depth survey by Kolmanovsky and McClamroch[3] on the broader topic of nonholonomic control, including the aspects of motion planning and geometric phases.

The focus of the present paper is on validation of the basics of the models and the corresponding multibody simulations by reproducing the results (assuming negligible flexibility) for a fully rigid system—namely that by Reyhanoglu and McClamroch[7]—and then demonstrating the effects of large flexible deflections on the reorientation manoeuvres. Whereas the authors' earlier work[11] considered a central hub with large and heavy appendages (all bodies identical), used multiple periodic loops in the shape space and commanded joint angle rates, the present work treats a more practical example with thinner appendages connected in a chain—hence affecting each other's motion—and uses a single rectangular shape profile, providing angular accelerations as inputs. This enables the comparison of the results against those of the existing literature. In addition, the present paper primarily focuses on the dynamics as opposed to the control aspect, as well as the dynamics' dependence on the system's configuration which becomes particularly important in the presence of flexibility.

Throughout this paper, a three-body system with a rigid hub and two flexible appendages, connected to each other in a chain format, is considered. It is assumed that the joint angles between the two appendages and between the hub and the inner appendage are controllable by applying known joint torques designed to achieve given joint angle

DOI: 10.13009/EUCASS2023-636

profiles. Section 2 discusses the required changes and additions to the models of Vatankhahghadim and Lovera[11] in order to make them applicable to the configuration of interest. Section 3 presents validation and simulation results for an attitude control problem using the torque functions designed by Reyhanoglu and McClamroch,[7] followed by a more detailed examination of the effects of flexibility and manoeuvre rate on the dynamics. Lastly, some concluding remarks are offered in Section 4.

2. Mathematical Models

This paper focuses on a three-body system with two slender appendages connected in a chain configuration—sharing a joint with each other—the inner one of which is also attached to a large rigid hub as shown in Figure 1. This allows comparing the results to those of Reyhanoglu and McClamroch,[7] and considering the current space applications and existing systems, could be viewed as a more realistic example than the one considered elsewhere by Vatankhahghadim and Lovera.[11] Most of the pertinent mathematical derivations and results for both rigid and flexible systems can be found in the authors' earlier work,[11] but because of the differences in their assumed multibody configurations and the fact that the flexible deflections in this case would now depend on each other—that is, the appendages are no longer only connected to the rigid hub, thus are not independent of each other—some changes are necessary and are briefly summarized in this section.

The first set of modifications to the models involves incorporating the motion of the inner appendage (directly connected to the hub) into the position, attitude, and velocity expressions of the second appendage:

$$\boldsymbol{\rho}_0^{02} = \boldsymbol{\rho}_0^{01} + L\begin{bmatrix}\cos\psi_1 & \sin\psi_2 & 0\end{bmatrix}^{\mathsf{T}} \tag{1a}$$

$$\boldsymbol{C}_{20} = \boldsymbol{C}_{21}\boldsymbol{C}_{10} = \boldsymbol{C}_{\mathrm{z}}(\psi_2)\boldsymbol{C}_{\mathrm{z}}(\psi_1) \tag{1b}$$

$$\boldsymbol{\omega}_2^{20} = \boldsymbol{\omega}_2^{21} + \boldsymbol{C}_{21}(\psi_2)\boldsymbol{\omega}_1^{10} \tag{1c}$$

where L is the appendages' length, $\boldsymbol{\rho}_0^{0j}$ contains the hub-frame components of the position vector from the hub's centre of mass to the joint of Body j, $\boldsymbol{C}_{ji}$ is the rotation matrix from frame $\mathscr{F}_i$ to frame $\mathscr{F}_j$, and $\boldsymbol{\omega}_j^{ji}$ represents the angular velocity of Body j relative to Body i as expressed in $\mathscr{F}_j$ denoted by the subscript. The joint angles ψ_1 and ψ_2 are those between Body 1 (the inner appendage) and the hub, and the two appendages, respectively.

In addition, because the appendages' shared joint position $\boldsymbol{\rho}_0^{02}$ is no longer fixed, its derivative should also be added to some of the rate expressions developed by Vatankhahghadim and Lovera.[11] For example, the position and velocity of the hub relative to the system's centre of mass as expressed in the hub's frame, denoted by $\boldsymbol{r}_{0,0}$ and $\dot{\boldsymbol{r}}_{0,0}$, now

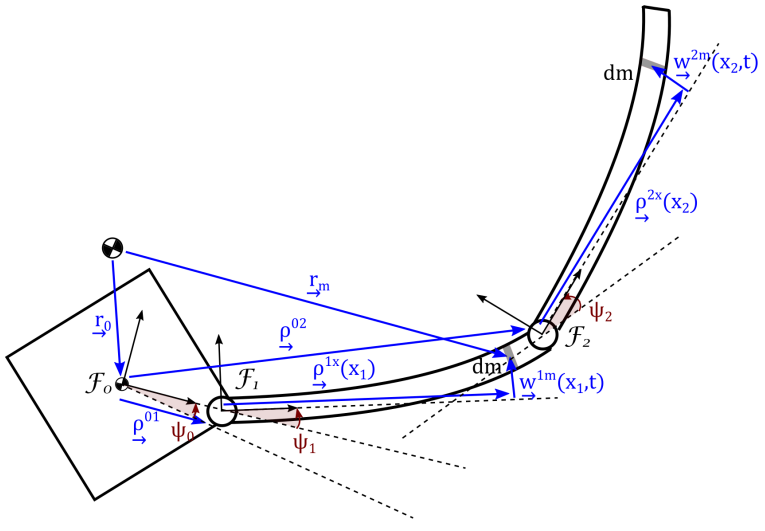

Figure 1: Sketch of the three-body system, with flexible appendages in a chain configuration

DOI: 10.13009/EUCASS2023-636

take the following forms:

$$\boldsymbol{r}_{0,0} = -\frac{1}{M}\sum_{j=1}^{2}\left[m_j\boldsymbol{\rho}_0^{0j} + \sigma\boldsymbol{C}_{0j}\int_0^L\left(\boldsymbol{\rho}_j^{jx} + \boldsymbol{w}_j^{jm}\right)\,dx_j\right] \tag{2a}$$

$$\dot{\boldsymbol{r}}_{0,0} = +\frac{1}{M}\sum_{j=1}^{2}\left[m_j\dot{\boldsymbol{\rho}}_0^{0j} + \sigma\boldsymbol{C}_{0j}\Big(\int_0^L\boldsymbol{\rho}_j^{jx}\,dx_j\Big)\boldsymbol{\omega}_j^{j0} + \sigma\boldsymbol{C}_{0j}\Big(\int_0^L\boldsymbol{w}_j^{jm}\,dx_j\Big)\boldsymbol{\omega}_j^{j0} - \sigma\boldsymbol{C}_{0j}\int_0^L\dot{\boldsymbol{w}}_j^{jm}\,dx_j\right] \tag{2b}$$

where $(\dot{\cdot})$ represents time derivative, m_j is the mass of Body j, $M \triangleq m_0 + m_1 + m_2$ is the total system mass, σ is the appendages' uniform linear density, and $\boldsymbol{w}_j^{jm}(x_j)$ is the point-wise flexible deflection of mass element dm at position x_j on Body j. Note the presence of the $\dot{\boldsymbol{\rho}}_0^{0j}$ term that would drop out the in the case of hub-fixed joints. A similar comment holds for the position and velocity of each mass element, $\boldsymbol{r}_{m,0}$ and $\dot{\boldsymbol{r}}_{m,0}$, which now should include the motion of the appendages relative to each other:

$$\boldsymbol{r}_{m,0} = \boldsymbol{r}_{0,0} + \boldsymbol{\rho}_0^{0j} + \boldsymbol{C}_{0j}\boldsymbol{\rho}_j^{jx} + \boldsymbol{C}_{0j}\boldsymbol{w}_j^{jm} \quad , \quad j \in \{1,2\} \tag{3a}$$

$$\dot{\boldsymbol{r}}_{m,0} = \dot{\boldsymbol{r}}_{0,0} + \dot{\boldsymbol{\rho}}_0^{0j} - \boldsymbol{C}_{0j}\left[(\boldsymbol{\rho}_j^{jx})^{\times} + (\boldsymbol{w}_j^{jm})^{\times}\right]\boldsymbol{\omega}_j^{j0} + \boldsymbol{C}_{0j}\dot{\boldsymbol{w}}_j^{jm} \quad , \quad j \in \{1,2\} \tag{3b}$$

where $(\cdot)^{\times}$ represents the cross product operator. Along with the position and velocity expressions in Eqs. (2) and (3), the system's angular momentum and energy expressions can be used to obtain its kinematics and dynamics models. For the purposes of this paper, only the dynamics model is required, and using a Largangian framework, the energy expressions would suffice to derive the system dynamics. After separating the flexible deflections into space- and time-varying parts as $\boldsymbol{w}_j^{jm} \triangleq \boldsymbol{W}_j(x_j)\boldsymbol{q}_j(t)$ and defining the overall system states as the complete set of generalized coordinates $\boldsymbol{x} \triangleq [\ \psi_1\ \psi_2\ \psi_0\ \boldsymbol{q}_1^{\mathsf{T}}\ \boldsymbol{q}_2^{\mathsf{T}}\ ]^{\mathsf{T}}$, the following equations of motion can be derived:

$$\boldsymbol{M}\ddot{\boldsymbol{x}} + \left(\dot{\boldsymbol{M}} + \boldsymbol{D}\right)\dot{\boldsymbol{x}} + \hat{\boldsymbol{k}} = \boldsymbol{\tau} \quad , \quad \hat{\boldsymbol{k}}(\boldsymbol{x},\dot{\boldsymbol{x}}) \triangleq -\dot{\boldsymbol{x}}^{\mathsf{T}}\frac{\partial \boldsymbol{M}}{\partial \boldsymbol{x}}\dot{\boldsymbol{x}} + \boldsymbol{K}\boldsymbol{x} \tag{4}$$

where $\boldsymbol{\tau}$ represents external torques, and $\boldsymbol{M}$, $\boldsymbol{K}$, and $\boldsymbol{D}$ are the system's overall mass, stiffness, and damping matrices, respectively. The nonlinear term $\hat{\boldsymbol{k}}$ captures both partial effects from the kinetic energy and the contribution of the strain energy due to the appendages' elasticity.

Numerical integration of Eq. (4), as is used in Section 3.1 below, provides a prediction of the system dynamics by generating time histories of the states: the joint angles, the attitude angle, and the deflection coordinates. It must be noted that the system matrices are state dependent, so they should be recomputed at each integration step using updated states. In this paper, commanded joint accelerations are assumed, namely specific $\ddot{\psi}_1$ and $\ddot{\psi}_2$ functions that would result in desired profiles for ψ and ψ_2 in the shape space, using which feedforward torques to be applied at the joints can be determined. The selection of the joint angle profiles is a design choice that involves consideration of how much attitude change they can offer and how achievable they would be in practical terms.

As a side note, the angular momentum expression mentioned earlier, together with the law of conservation of angular momentum that would require such an expression to remain zero in the absence of any external torques, would prove useful for controller design and computing the geometric phases as was done by Walsh and Sastry,[12] for example: given that the angular momentum is related to the angular velocity and deflection rate terms—that is, $\boldsymbol{h} = \boldsymbol{J}^{\mathsf{T}}\dot{\boldsymbol{x}}$, where $\boldsymbol{J}$ generically represents the state-dependent coefficients corresponding to each rate term—setting it to zero and integrating the result over time would offer a correlation between the attitude changes—called "geometric phase", the difference $\psi_0(t_f) - \psi_0(t_i)$ between the attitude angle at some initial and final times, t_i and t_f—and those of the joint angles and deflection coordinates (via $\dot{\psi}_1$, $\dot{\psi}_2$, $\dot{\boldsymbol{q}}_1$, and $\dot{\boldsymbol{q}}_2$). Interested readers are referred to Vatankhahghadim and Lovera[11] for more details on this approach in the presence of flexibility, as well as for each term and the general form of the expressions in Eq. (4)—which would be similarly applicable to this paper's models—as the rest of this document is focused on the simulations and the effects of flexibility and appendage configuration on the dynamics.

3. Simulation Results

A numerical example and some simulation results are presented in this section. Section 3.1 uses the same shape space profile and nearly rigid appendages to compare the results against those previously reported by Reyhanoglu and McClamroch,[7] while Section 3.2 uses a simpler profile to focus on the effects of appendage flexibility of various amounts on the attitude control manoeuvre.

DOI: 10.13009/EUCASS2023-636

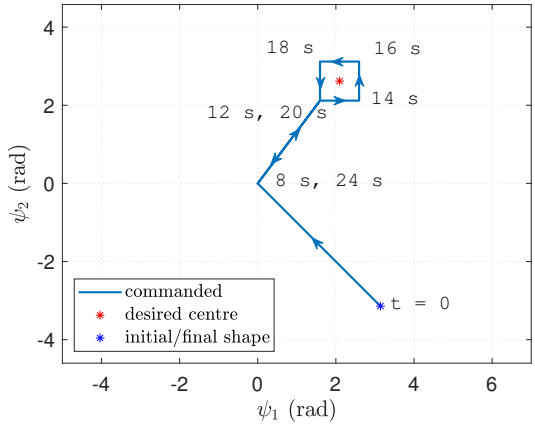

Figure 2: Shape space profile obtained using the joint accelerations designed by Reyhanoglu and McClamroch[7]

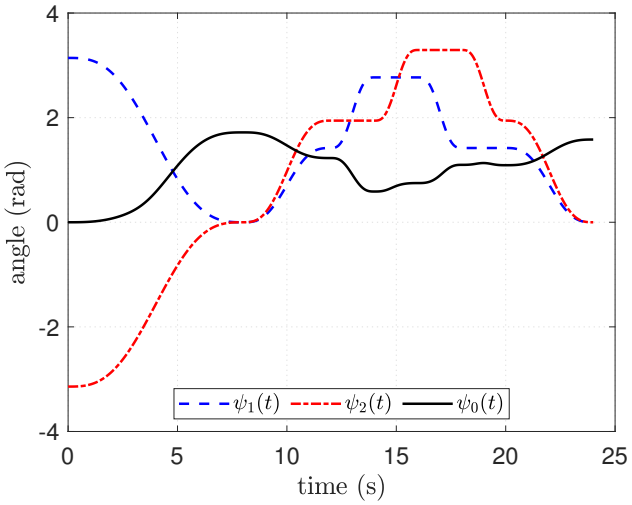

Figure 3: Time history of the joint and attitude angles of the rigid system in response to the shape space profile in Figure 2

Consistent with the geometrical and physical parameters used by Reyhanoglu and McClamroch,[7] a square-shaped "planar" rigid hub of mass 120 kg and diameter 1 m, and negligible thickness 0.01 m; and two slender appendages of mass 12 kg, length 1 m and cross-sectional square side length 0.01 m are assumed. For the flexible appendages, structural damping with mass and stiffness proportionality coefficients of 1 s^{-1} and 1 s, respectively, are used. The appendages' Young's modulus is varied in Section 3.2 to simulate various degrees of flexibility.

3.1 Validation against Past Results

In this section, the results from Reyhanoglu and McClamroch[7] are reproduced for a fully rigid system, using the same joint acceleration profiles. Applying the changes described in this paper to the models of Vatankhahghadim and Lovera,[11] the attitude changes of a completely rigid three-body system—which could also be viewed as a limiting case of having negligible flexibility—are simulated. Shown in Figure 2 is the shape space profile used, which illustrates the evolution of the joint angles: starting from their initial configuration, $(\psi_1, \psi_2) = (\pi, -\pi)$ shown by a blue asterisk, completing a square path centred at $(2\pi/3, 5\pi/6)$—selected based on a study of how much change in attitude can be obtained by changing the joint angles in the vicinity of such a centre—and back to the final configuration at $(0, 0)$. The reader is referred to Reyhanoglu and McClamroch[7] for the complete set of piece-wise acceleration terms used to obtain such a profile, but to illustrate what such control functions could look like, the following is a possible choice for the joint accelerations to take an initial $\boldsymbol{\psi}_i \triangleq [\ \psi_1(t_i)\ \psi_2(t_i)\ ]^\mathsf{T}$ at time t_i to a final $\boldsymbol{\psi}_f$ at t_f for a given segment in the shape

DOI: 10.13009/EUCASS2023-636

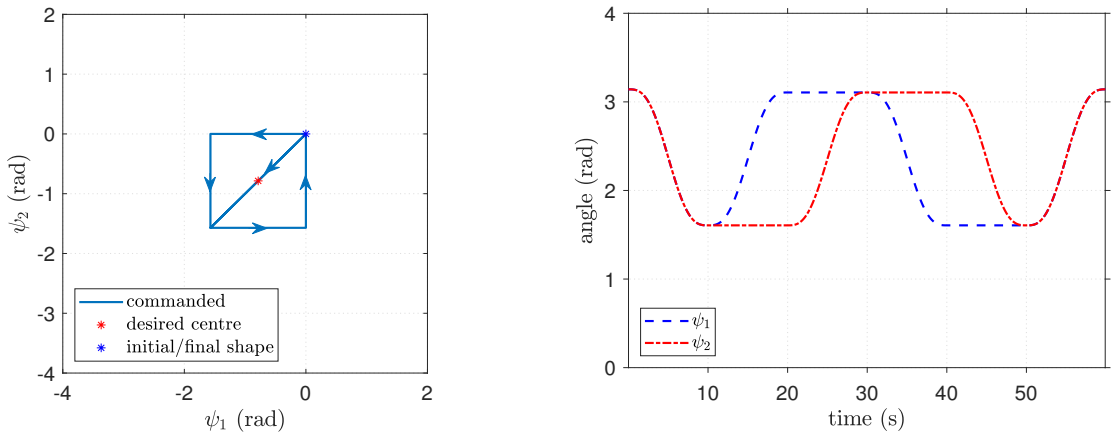

(a) (b)

Figure 4: Profile used for the flexible system, using the joint acceleration functions proposed by Reyhanoglu and McClamroch:[7] (a) shape space representation and (b) time-domain representation

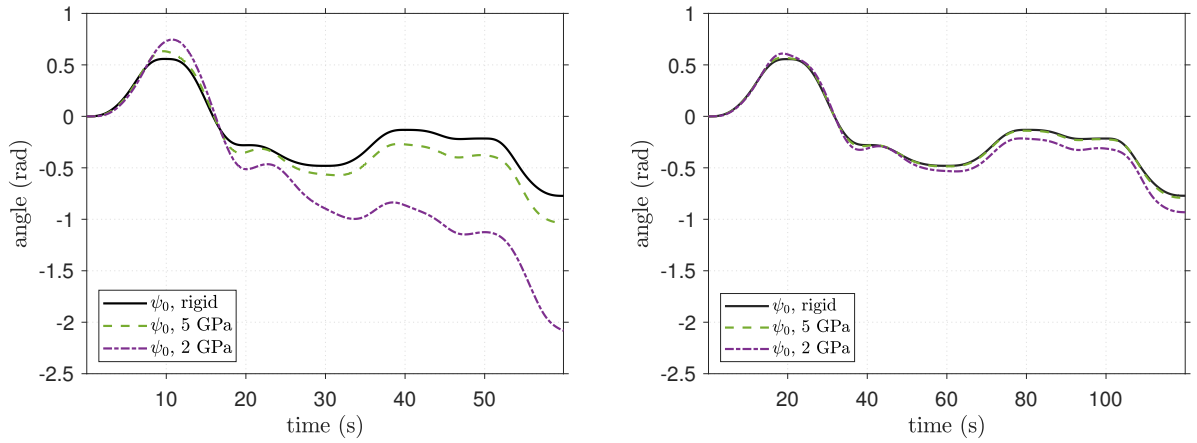

(a) (b)

Figure 5: Time history of the joint and attitude angles of the flexible system in response to the shape space profile in Figure 4 (a) completed in 60 s and (b) completed in 120 s

space defined by the joint angles:[7]

$$\ddot{\boldsymbol{\psi}}(t) = \frac{2\pi(\boldsymbol{\psi}_f - \boldsymbol{\psi}_i)}{(t_f - t_i)^2} \sin\left[\frac{2\pi(t - t_i)}{t_f - t_i}\right] \quad , \quad t \in [t_i, t_f) \tag{5}$$

In short, the overall idea is completing each segment using a smooth profile—starting and ending with zero accelerations—and traversing the desired square path that physically implies keeping one of the angles constant while increasing or decreasing the other one. The side-length of the square path is set to $z^* = 1.35$ rad in this case. It should be noted that the various results obtained by Reyhanoglu and McClamroch[7] and their comparison suggest that their joint angle ψ_2 is measured from the outer to the inner appendage, so the same definition is assumed in this section—in contrast to the definitions in Figure 1, which are in the opposite direction and are retained in the subsequent sections' simulations.

The time histories of the joint and attitude angles are shown in Figure 3, obtained by numerically integrating the system dynamics in Eq. (4), and offer a good match with the time responses provided in Figure 4 of the paper by Reyhanoglu and McClamroch.[7] This adds another layer of validation for the formulation of Vatankhahghadim and Lovera[11]—albeit for a different configuration and circular profiles, and rate-based as opposed to acceleration control inputs—and provides a reliable foundation for studying the flexibility effects in the subsequent section.

DOI: 10.13009/EUCASS2023-636

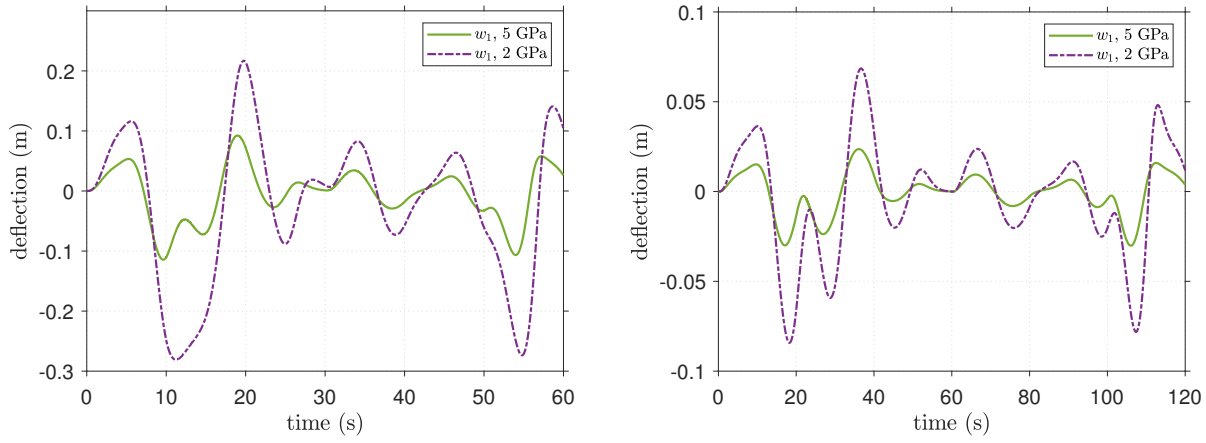

Figure 6: Time history of the flexible deflections of the first (inner) appendage in response to the shape space profiles in Figure 4: (a) completed in 60 s and (b) completed in 120 s

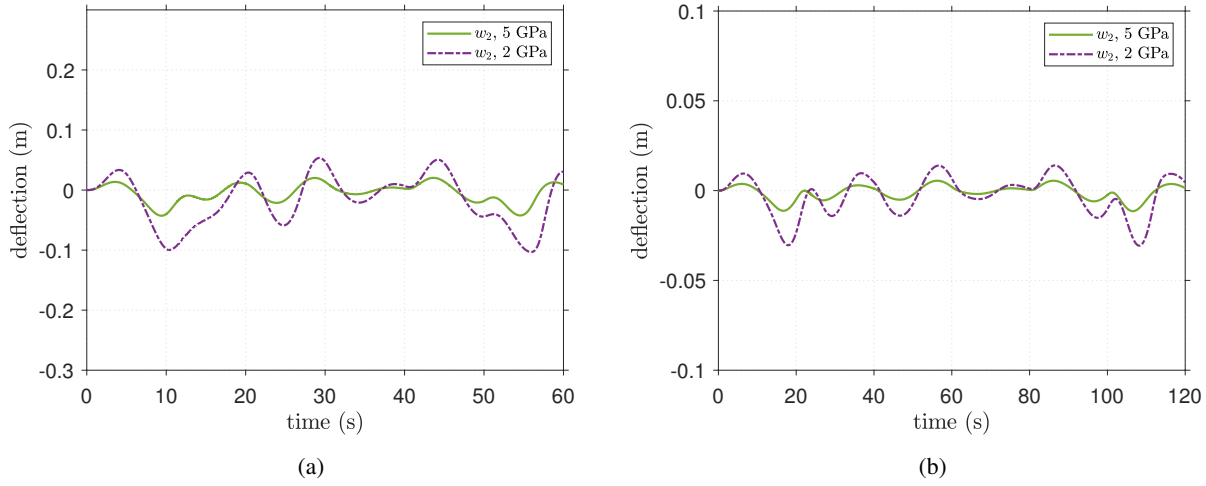

Figure 7: Time history of the flexible deflections of the second (outer) appendage in response to the shape space profiles in Figure 4: (a) completed in 60 s and (b) completed in 120 s

3.2 Effects of Flexibility

A slightly simpler and larger profile, as shown in Figure 4 and consistent with the definitions in Figure 1, is used to illustrate the effect of flexibility on the attitude change as a result of appendage motions. The square path in the shape space, represented in Figure 4a, is assigned a length of $z^* = 1.5$ rad. The resulting joint angles (in dashed blue and dash-dotted red curves for the inner and outer appendages, respectively) are shown in Figure 4b. The attitude angle history, produced by a Simscape™ simulation of the system, is shown in Figure 5 for three cases: near-rigid appendages (with a very large modulus of flexibility) in solid black, appendages with Young's modulus $E = 5$ GPa in dashed green, and appendages with $E = 2$ GPa in dash-dotted purple. Separate results are provided for different rates of traversing the shape space profile: in 1 minute, as in Figure 5a, or in 2 minutes, resulting in the dynamics in Figure 5b.

Also examined in this section are the appendages' flexible deflections, presented in Figures 6 and 7, using solid green and dash-dotted purple curves to identify the cases with $E = 5$ GPa and $E = 2$ GPa, respectively. Figures 6a and 6b show the deflections of the first (inner) appendage, with each subplot corresponding to a different manoeuvre rate (completed in 60 s or 120 s), while Figures 7a and 7b do the same for the second (outer) appendage. As evident from the results, even relatively small flexibility effects that cause deflections of no more than around 0.2 m—for 10 m long appendages—can have a significant effect on the resulting attitude changes, in these cases up to ~ 1.3 rad in the 1-minute simulation of Figure 5a with $E = 2$ GPa.

DOI: 10.13009/EUCASS2023-636

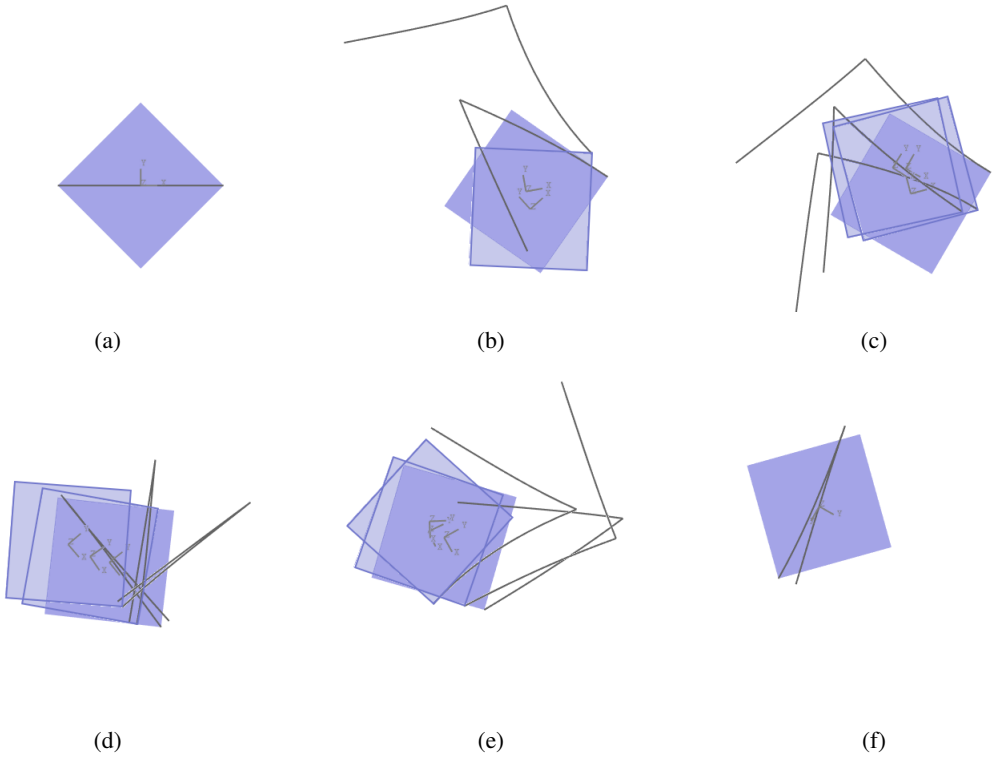

Figure 8: Snapshots of the attitude change maneouvre, with 5 s intervals (with darker hubs corresponding to the starting times of each interval), at times: (a) 0 s, (b) 5–10 s, (c) 15–25 s, (d) 30–40 s, (e) 45–55 s, and (f) 60 s

Comparing Figure 5a against 5b suggests an intuitive and simple way to alleviate such unwanted effects in real applications: using slower manoeuvres that minimize the flexible deflections, hence making the actual dynamics more in line with the rigid-based predictions. For example, with the overall manoeuvre time in Figure 5b being twice as much as that in Figure 5a, the discrepancy (relative to the rigid case) between the final attitude in the case with the appendages having $E = 2$ GPa is reduced to ~ 0.16 rad, and the attitude pattern for the system with $E = 5$ GPa becomes virtually identical to that of the rigid case. It is also interesting to contrast the flexible deflection patterns in Figures 6a and 7a against those in Figures 6b and 7b: the resulting patterns of their troughs and crests are quite similar, with the magnitudes in the first pair of subplots being about three times larger than the corresponding ones among the latter pair with a slower manoeuvre.

Lastly, presented in Figure 8 are snapshots of the motion for the case with $E = 2$ GPa and using the profile in Figure 4a traversed in 1 minute. This figure illustrates the attitude change manoeuvre achieved by actuating the joints, and shows the effects of flexibility that induces curves in the appendages during the manoeuvre, subsequently affecting the main hub's rotational and translational motions. The initial and final configurations are shown in Figures 8a and 8f, respectively: in the absence of flexibility, rigid appendages would be aligned along the hub's diagonal also in the final configuration, but now they have clear deflections that will eventually die out over time, depending on the structural damping. Another observation is how the deflections of the inner appendage affect the motion of the outer one: an aspect that would not be present in the previous example considered by the present authors,[11] in which the appendages are connected separately to the central hub. This highlights that importance of the system configuration, and how the influence of flexibility on the dynamics can be augmented or diminished depending on the structural design.

4. Conclusion

This paper focuses on the effects of flexibility on attitude control manoeuvres performed by actuating the internal joints of multibody spacecraft to change their shape. As a continuation of the earlier work by Vatankhahgahdim and Lovera,[11] the necessary changes in the mathematical models are presented to render them applicable to the chained configuration of interest (as opposed to having a central hub); however, most of the simulation results involving flexibility are obtained using built-in multibody models—in turn verified against the predictions using the developed mathematical

DOI: 10.13009/EUCASS2023-636

models. The numerical example, joint angle profiles, and commanded torques presented by Reyhanoglu and McClamroch[7] are then used to validate the model if the appendage were rigid. Lastly, to assess how various amounts of appendage flexibility would affect the attitude control manoeuvre, a simpler square-shaped profile is selected and the system's attitude angle, flexible deflections, and overall planar motion are examined. It is observed that repeating the same manoeuvre at a slower rate can significantly contribute to minimizing the amount of deflections, as well as the subsequent attitude deviations.

It is clear that even small amounts of flexibility can have a significant impact on the system's motion during the attitude change manoeuvre. Some considerations and an approach to correct the attitude prediction using geometric phases—based on the rigid dynamics—are presented elsewhere by the current authors,[11] but more work would be required to render such approaches more general, encompassing situations such as those involving the configuration in this paper, or spacecraft with more than two appendages—some of which may inevitably be linked in a direct manner, hence mutually affecting each other's motion. Nevertheless, having verified in this paper the basics of the models against the results of Reyhanoglu and McClamroch,[7] and subsequently having assessed the effects of varying the rigidity and maneouvre times in simple and representative cases, future work in the aforementioned directions can ensue to more systematicaly and comprehensively account for flexibility in attitude control via shape change.

5. Acknowledgments

This research is partially supported by the Natural Sciences and Engineering Research Council of Canada through its Postdoctoral Fellowships program.

References

[1] W. T. Cerven and V. L. Coverstone. Optimal reorientation of a multibody spacecraft through joint motion using averaging theory. *Journal of Guidance, Control, and Dynamics*, 24(4):788–795, 2001.

[2] T. R. Kane and M. P. Scher. A dynamical explanation of the falling cat phenomenon. *International Journal of Solids and Structures*, 5(7):663–670, 1969.

[3] I. Kolmanovsky and N. H. McClamroch. Developments in nonholoomic control problems. *IEEE Control Systems Magazine*, 15(6):20–36, 1995.

[4] P. S. Krishnaprasad. Geometric phases and optimal reconfiguration for multibody systems. In *Proceedings of the American Control Conference*, pages 2440–2444, San Diego, CA, 1990.

[5] P. S. Krishnaprasad and R. Yang. Geometric phases, anholonomy, and optimal movement. In *Proceedings of the 1991 IEEE International Conference on Robotics and Automation*, pages 2185–2189, Sacramento, CA, 1991.

[6] T. Narikiyo and M. Ohmiya. Control of a planar space robot: Theory and experiments. *Control Engineering Practice*, 14(875-883):8, 2006.

[7] M. Reyhanoglu and N. H. McClamroch. Planar reorientation maneuvers of space multibody systems using internal controls. *Journal of Guidance, Control, and Dynamics*, 15(6):1475–1480, 1992.

[8] C. Rui, I. V. Kolmanovsky, and N. H. McClamroch. Nonlinear attitude and shape control of spacecraft with articulated appendages and reaction wheels. *IEEE Transactions on Automatic Control*, 45(8):1455–1469, 2000.

[9] N. Sreenath. *Modeling and Control of Multibody Systems*. PhD thesis, University of Maryland, College Park, MD, 1987.

[10] N. Sreenath. Nonlinear control of planar multibody systems in shape space. *Mathematics of Control, Signals, and Systems*, 5(4):343–363, 1992.

[11] B. Vatankhahghadim and M. Lovera. Attitude control of flexible multibody spacecraft via shape change. submitted to *Journal of Guidance, Control, and Dynamics*, 2023.

[12] G. C. Walsh and S. S. Sastry. On reorienting linked rigid bodies using internal motions. *IEEE Transactions on Robotics and Automation*, 11(1):139–146, 1995.